Received: 19 December 2019 | Revised: 2 March 2020 | Accepted: 9 March 2020

DOI: 10.1002/jhet.3972

Check for updates

WILEY

ARTICLE

Design, synthesis, and biological evaluation of sorafenib derivatives containing indole (ketone) semicarbazide analogs as antitumor agents

Wen Li[1] | **Ya-Yun Qi**[1] | **Yuan-Yuan Wang**[1] | **Yi-Yuan Gan**[1] | **Li-Hui Shao**[1] | **Li-Qiong Zhang**[1] | **Zhen-Hua Tang**[1] | **Mei Zhu**[1] | **Si-Yu Tang**[1] | **Zhen-Chao Wang**[1] | **Gui-Ping Ouyang**[1,2,3]

[1]School of Pharmaceutical Sciences, Guizhou University, Guiyang, People's Republic of China

[2]State Key Laboratory of Functions and Applications of Medicinal Plants, Guizhou Medical University, Guiyang, People's Republic of China

[3]Guizhou Engineering Laboratory for Synthetic Drugs, Guiyang, People's Republic of China

Correspondence
Zhen-Chao Wang and Gui-Ping Ouyang, School of Pharmaceutical Sciences, Guizhou University, Huaxi District, Guiyang, Guizhou Province, 550025, People's Republic of China.
Email: wzc.4884@163.com (Z.-C. W) and oygp710@163.com (G.-P. O.)

Funding information
the National Natural Science Foundation of China, Grant/Award Number: 21867004; the project of State Key Laboratory of Functions and Applications of Medicinal Plants, Guizhou Medcial University, Grant/Award Number: FAMP201707K; the Science Technology Program of Guizhou province, Grant/Award Number: 20185781

Abstract

A series of new sorafenib derivatives was designed and synthesized. The antiproliferative activity of the synthesized compounds against human lung cancer cell (A549), human pancreatic cancer cell (PC-3), human leukemia cell (K562), and human hepatoma cell (SMMC-7721) was evaluated by MTT assay. The results revealed that several compounds displayed more significant antitumor activities than commercial anticancer agent sorafenib against SMMC-7721. In addition, compounds **7a**, **7g**, **7l**, **7m**, and **7p** represented obvious growth inhibition with IC_{50} values of 1-9 μM against four cancer cell lines, demonstrating more predominant activities against cancer cells as compared to sorafenib. Furthermore, some structure-activity relationships have also been established. Compounds containing indole and benzene ring substituted by halogen showed better activity than sorafenib. Wound healing assay suggested that cells would be targeted on their migratory capacity by **7g**, potentially affecting the migration activity of these tumors. The effects of A549 and PC-3 cell apoptosis induced by compound **7g** were significantly increased compared with sorafenib. Importantly, the result of western blot assay showed that **7g** inhibited cell growth by suppressing the activity of EGFR, especially the expression of p-EGFR (Tyr1068).

1 | INTRODUCTION

Sorafenib, a diaryl urea multiple-targeted antitumor agent, jointly developed by Bayer and Onyx, US, was proved to inhibit kinases including Raf, VEGFR, PDGFR, and KIT involved in tumor proliferation and angiogenesis.[1,2] Recently, sorafenib was proved to be effective for the treatment of non-small cell lung cancer, breast cancer, and thyroid cancer.[3–5] At present, there are three ways by which sorafenib fights against cancer. First, sorafenib blocks cancer cell proliferation by inhibiting BRaf and Raf 1/c-Raf kinase phosphorylation in the protein kinase pathway. Second, sorafenib prevents tumor-associated angiogenesis by inactivating vascular endothelial growth factor

Wen Li and Ya-Yun Qi contributed equally to this work.

 © 2020 Wiley Periodicals, Inc.

receptors (VEGFR), the platelet-derived growth factor receptor-β (PDGFR-β) and stem cell growth factor receptor (c-kit). Third, sorafenib induces tumor cell apoptosis by reducing elF4E phosphorylation and downregulating Mcl-1 levels.[6–14] Sorafenib has been proven to be of broad spectrum and well tolerated, but due to the various side effects of sorafenib, it is necessary to explore for new antitumor drugs with high efficiency and low toxicity.

In most studies including our previous work, it was found that indole constituted various compounds with superior antitumor activity. It is known that indole is versatile and privileged in drug discovery,[15–18] such as the nintedanib for the treatment of idiopathic pulmonary fibrosis (IPF),[19] the vinorelbine for the treatment of non-small cell lung cancer and breast cancer,[20] acemetacin for the treatment of rheumatoid arthritis,[21] and sunitinib for the treatment of renal cancer and gastrointestinal stromal tumors (Figure 1).[22] A series of indole vinyl sulfones compounds were reported by Li in 2019; the bioassay showed that compound A presented potent activity against HepG2, A549, and K562 (Figure 1).[23] Especially, derivatives bearing amino and ureide moiety based on indole scaffold usually have noteworthy antitumor activity, for example, compound B (Figure 1) was reported by Eldehna in 2019, which emerged as the most potent multikinase inhibitor in the ureido analogues series with VEGFR-2, FGFR-1, and PDGFR-b IC_{50} of 0.18, 0.23, and 0.10 μM, respectively. And it was also very effective toward HepG2 cells ($IC_{50} = 2.67 \pm 0.14$ μM) and A498 cells ($IC_{50} = 1.00 \pm 0.02$ μM).[24]

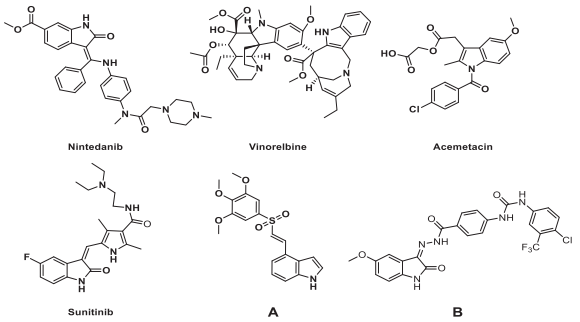

FIGURE 1 Structures of indole derivatives

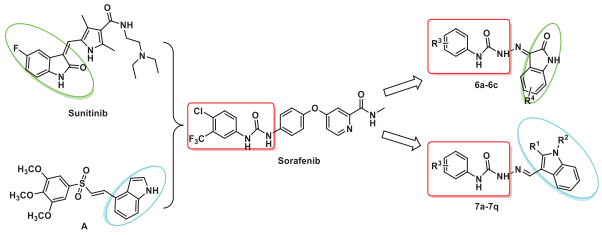

FIGURE 2 Design idea of the target compounds

On the basis of the previous considerations and our high interest at the development of sorafenib and indole, a series of new sorafenib derivatives were designed and synthesized by substituting semicarbazide indole derivatives for urea (Figure 2).

2 | RESULTS AND DISCUSSION

2.1 | Chemistry

The synthesis route of the target molecules **6a–c** and **7a–q** was outlined in Scheme 1. 1*H*-indole-3-carbaldehyde (**1a**) was prepared via a one-step procedure that involved the

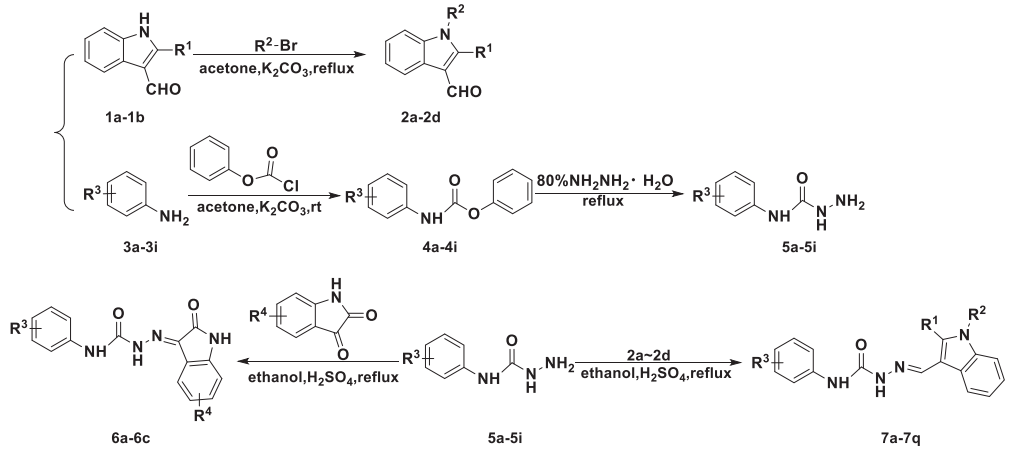

6a: R^3=3-CF_3,4-Cl, R^4=H; **6b**: R^3=3-F,4-F, R^4=H; **6c**: R^3=3-CF_3,4-Cl, R^4=5-CH_3; **7a**: R^1=H, R^2=H, R^3=3-Br; **7b**: R^1=H, R^2=H, R^3=3-F, 4-F;
7c: R^1=H, R^2=H, R^3=3-CF_3, 4-Cl; **7d**: R^1=H, R^2=H, R^3=4-CH_3; **7e**: R^1=Cl, R^2=H, R^3=3-F, 4-F; **7f**: R^1=Cl, R^2=H, R^3=3-Cl;
7g: R^1=Cl, R^2=H, R^3=3-Br; **7h**: R^1=Cl, R^2=H, R^3=4-OCH_3; **7i**: R^1=Cl, R^2=H, R^3=3-CF_3, 4-Cl; **7j**: R^1=Cl, R^2=CH_2CH_3, R^3=3-CF_3, 4-Cl;
7k: R^1=Cl, R^2=CH_2CH_3, R^3=4-F; **7l**: R^1=Cl, R^2=CH_2CH_3, R^3=3-Br; **7m**: R^1=Cl, R^2=CH_2CH_3, R^3=2-F; **7n**: R^1=Cl, R^2=CH_2CH_3, R^3=3-F;
7o: R^1=Cl, R^2=CH_2CH_3, R^3=4-OCH_3; **7p**: R^1=Cl, R^2=CH_2CH_3, R^3=3-Cl; **7q**: R^1=Cl, R^2=$CH_2CH_2CH_3$, R^3=3-Br.

SCHEME 1 Synthetic routes of the target compounds **6a–c** and **7a–q**

Vilsmeier–Hacck reaction of 1*H*-indole with acylation agent DMF under the $POCl_3$ catalyzing to give.[25] Similarly, 2-chloro-1*H*-indole-3-carbaldehyde (**1b**) was synthesized according to a method previously reported in the literature.[26] Molecules **5a–i** were selected as our key intermediates for this series of reactions, and were synthesized by means of a two-step procedure that involved the substitution reaction of substituted aniline **3a–i** with phenyl carbonochloridate to give carbonate compounds **4a–i**, which were then reacted with 80% hydrazine.[27] One of the objectives of this study was the preparation of target compounds **6a–c** and **7a–q**, a structure analogue of sorafenib. Preparation of *N*-(substituted phenyl)-2-(2-oxoindolin-3-ylidene)hydrazine-1-carboxamide **6a–c** and 2-((substituted 1*H*-indol-3-yl) methylene)-*N*-(substituted phenyl)hydrazine-1-carboxamide **7a–q** was accomplished via the condensation reaction of substituted isatin or **2a–d** with semicarbazide compounds **5a–i**.

The structures of **6a–c** and **7a–q** were characterized and confirmed by means of ^{1}H NMR, ^{13}C NMR, and HRMS spectra. The characteristic hydrogen atoms of the target compounds were affiliated to the ^{1}H NMR spectrum as follows. The ^{1}H NMR spectra of **7a–i** revealed the presence of singlet signals at δ 12.40-11.52 ppm corresponding to indole-NH protons; the ^{1}H NMR spectra of **6a–c** and **7a–i** manifested the existence of CONHN and PhNHCO singlet signals at around δ 10.88-10.39 ppm and δ 9.96-8.41 ppm, respectively. Whereas the ^{1}H NMR spectra of compounds **6a–c** showed indolone-NH single peaks at around δ 10.56-10.50 ppm, and the ^{1}H NMR spectra of compounds **7a–q** showed N═CH single peaks at about δ 8.25-8.16 ppm, and the ^{1}H NMR spectra of compounds **7a–d** showed indole-2-H double peaks at about δ 7.84-7.79 ppm. Additionally, the quartets at δ 4.33-4.31 ppm was assigned to the methylene group on NCH_2CH_3 of target molecules **7j–p**. The triplet at δ = 4.26 ppm was designated to the first methylene group on $NCH_2CH_2CH_3$ of compounds **7q**; the single peaks at δ = 3.74 ppm came under the jurisdiction of the signal of three hydrogens on Ph-OCH_3 of **7h** and **7o**; the single peaks at δ 2.33-2.27 ppm belonged to Ph-CH_3 resonances of **6c** and **7d**; the multiple peaks at δ 1.83-1.70 ppm were the two hydrogen signals of the second methylene group on $NCH_2CH_2CH_3$ of **7q**; and the triplets at δ 1.30-0.87 ppm were the three hydrogen signals of the methyl group on CH_2CH_3 of **7j–q**. Likewise, the characteristic carbon atoms of the target compounds were attached to the ^{13}C NMR spectrum as follows. The ^{13}C NMR spectra of compounds **6a–c** showed the chemical shift of indole-2-carbonyl carbon at about δ 165.22-165.06 ppm, the ^{13}C NMR spectra of **6a–c** and **7a–i** manifested the existence of NHCONH signal at around δ 153.69-152.75 ppm, and the ^{13}C NMR spectra of **6a**, **6c**, **7c**, **7i**, and **7j** disclosed the $PhCF_3$ quartets at around δ 123.42-123.01 ppm, whose coupling constant is calculated manually. Furthermore, the measured value of HRMS $[M+H]^+$, $[M+Na]^+$, or $[M-H]^+$ of the target compounds were consistent with the theoretical value, and the errors were within m/z ± 0.005, which further confirmed the structures of the target compounds. Finally, the melting point determination of the target molecules indicated the melting point range of indolone semicarbazide sorafenib analogues **6a–c** at about 250°C-261°C, while that of the indole semicarbazide sorafenib derivatives **7a–q** was around 193°C-237°C.

2.2 | MTT assay

The antitumor activities against four cell lines of all of the synthesized compounds were evaluated using sorafenib as positive control. The results for the inhibitions rate of the derivatives are listed in Table 1. The IC_{50} (dose of the compound that caused a 50% reduction of survival values) are shown in Table 2. From the analysis of Table 1, at the concentration of 10 μM, the great majority of compounds exhibited comparable or even better antitumor activity against the four cell lines. For example, compounds **6a**, **7a**, **7g**, **7j**, **7l**, **7m**, **7n**, and **7q** had the inhibition rates of 51.39 ± 3.39%, 57.45 ± 2.32%, 67.05 ± 3.82%, 59.71 ± 3.81%, 55.45 ± 3.62%, 68.69 ± 1.45%, 46.52 ± 4.09%, and 57.63 ± 0.06% against A549, PC-3, SMMC-7721, and K562 respectively, which was more active than the control sorafenib (35.30 ± 3.45%, 41.95 ± 1.84, 38.34 ± 8.86, and 48.25 ± 1.08 against A549, PC-3, SMMC-7721, and K562 respectively). Additionally, compounds **7a**, **7g**, **7l**, **7m**, and **7p** possessed excellent antitumor activity against PC-3, with the inhibition rates of 55.21 ± 6.35%, 50.49 ± 6.84%, 58.03 ± 3.06%, 56.32 ± 5.60%, and 58.81 ± 0.71%, respectively, compared with the control sorafenib. As for the K562, compounds **7a**, **7g**, **7l**, **7m**, **7n**, and **7p** were found to possess better inhibition activities than positive control. Even better, most of compounds possessed more potency in antiproliferation effect against SMMC-7721.

According to the inhibition rate results of the target compounds **6a–c** and **7a–q** against four cancer cell lines (Table 1), we picked 16 compounds with high inhibition of cancer cells and measured their IC_{50} values. As shown in Table 2, all of the test compounds had excellent activities with the IC_{50} values ranging from 28.76 ± 3.72 to 4.08 ± 1.21 μM against A549, from 46.91 ± 1.99 to 3.53 ± 0.44 μM against PC-3, from 13.95 ± 2.89 to 1.73 ± 0.25 μM against SMMC-7721, from 116.25 ± 1.91 to 1.43 ± 0.14 μM against K562, which showed better antitumor activities than sorafenib (IC_{50} = 23.01 ± 1.33 μM against A549, 16.69 ± 4.44 μM

TABLE 1 Antitumor activities of the tested compounds using MTT assay on the four cell lines at 10 μM

Compound	Inhibition rate (%)[a] ± SD			
	A549	PC-3	SMMC-7721	K562
6a	51.39 ± 3.39	21.53 ± 3.15	24.65 ± 0.95	22.07 ± 6.38
6b	8.01 ± 1.14	20.27 ± 0.05	57.14 ± 1.87	16.95 ± 2.28
6c	17.02 ± 3.99	19.96 ± 2.72	51.77 ± 6.97	15.63 ± 9.54
7a	57.45 ± 2.32	55.21 ± 6.35	58.72 ± 1.06	87.35 ± 0.37
7b	17.11 ± 1.62	25.45 ± 9.16	22.27 ± 3.77	23.43 ± 7.12
7c	21.67 ± 5.84	15.90 ± 0.96	26.03 ± 6.51	24.29 ± 2.62
7d	7.11 ± 3.19	4.95 ± 2.70	7.61 ± 8.93	13.00 ± 5.24
7e	8.15 ± 8.63	33.63 ± 4.82	66.80 ± 3.13	6.84 ± 2.14
7f	38.13 ± 6.76	32.47 ± 7.59	45.27 ± 6.83	31.00 ± 2.94
7g	67.05 ± 3.82	50.49 ± 6.84	67.64 ± 0.67	88.65 ± 1.15
7h	25.29 ± 3.82	18.34 ± 8.50	32.62 ± 3.42	24.72 ± 2.83
7i	8.63 ± 1.28	24.11 ± 3.08	30.12 ± 9.58	19.77 ± 6.12
7j	59.71 ± 3.81	13.86 ± 7.88	63.41 ± 3.77	43.65 ± 3.92
7k	30.08 ± 3.29	26.09 ± 3.74	52.77 ± 1.14	13.81 ± 6.25
7l	55.45 ± 3.62	58.03 ± 3.06	67.12 ± 5.36	75.53 ± 1.97
7m	68.69 ± 1.45	56.32 ± 5.60	69.03 ± 4.95	82.76 ± 1.08
7n	46.52 ± 4.09	17.08 ± 7.60	72.09 ± 1.24	70.00 ± 3.55
7o	33.26 ± 6.75	35.30 ± 3.92	58.24 ± 1.84	14.97 ± 0.66
7p	32.75 ± 2.31	58.81 ± 0.71	66.01 ± 0.81	75.55 ± 3.16
7q	57.63 ± 0.06	26.27 ± 4.92	65.16 ± 1.49	22.76 ± 2.22
Sorafenib[b]	35.30 ± 3.45	41.95 ± 1.84	38.34 ± 8.86	48.25 ± 1.08

[a]The average of three trials.
[b]Commercial sorafenib was used as positive control.

against PC-3, 13.62 ± 0.52 μM against SMMC-7721 and 12.33 ± 2.52 μM against K562). Interestingly, compounds **7a**, **7g**, **7l**, **7m**, and **7p** showed superb IC_{50} values against the four cell lines in vitro, respectively.

Based on the analysis of the anticancer activity of the compounds obtained by changing the types and positions of the substituents, a structure-activity relationship was preliminarily established. First, it was found that compounds containing indolyl showed more significant antitumor activities than those containing the indole ketone group. Second, the substitutions on the benzene ring were important to their inhibition activities against the four cell lines. For example, compounds substituted by electron-donating (eg, $-CH_3$ and $-OCH_3$) compounds, such as **7d**, **7o**, and **7h**, and the substitution of trifluoromethyl and chlorine-containing (eg, **7c**, **7i**, and **7j**) compounds, exerted weaker inhibition activities than the others. However, compounds substituted by halogen (eg, **7m** containing fluorine, **7p** containing chlorine, **7a** containing bromine) showed better cytotoxicity than sorafenib. Further, compounds **7a** (3-Br), **7g** (3-Br), and **7l** (3-Br) gave the marked activity than **7m** (1-F), **7n** (2-F), and the inhibition activity of compounds substituted by chlorine was the least. From the comparison between compounds **7m**, **7n**, and **7k**, the ortho-substitution performed prominent activity than meta-substitution and para-substitution, which possessed the least activity. Third, the structural change at R_2 appeared to have a considerable effect on the anticancer activity. From comparison of compounds **7g** (R_2 = -H), **7l** (R_2 = $-CH_2CH_3$) and **7q** (R_2 = $-CH_2CH_2CH_3$), it was obvious that compound **7g** (IC_{50}: 4.93 ± 1.69 μM, 3.53 ± 0.44 μM, 5.48 ± 0.81 μM, and 1.43 ± 0.14 μM against the four cell lines, respectively) showed better comparable cytotoxicity than **7l** (IC_{50}: 8.99 ± 2.60 μM, 7.72 ± 0.76 μM, 2.97 ± 0.65 μM, and 2.25 ± 0.31 μM against the four cell lines, respectively) and compound **7q** (IC_{50}: 6.89 ± 0.86 μM against A549, 1.73 ± 0.25 μM against SMMC-7721).

2.3 | Wound healing assay

The role of target compounds at 5 μM in A549 cell migration was assessed using a wound healing assay.

TABLE 2 Anticancer IC_{50} values of the tested compounds using MTT assay on the four cell lines

Compound	IC_{50} (μM)[a] ± SD			
	A549	PC-3	SMMC-7721	K562
6a	11.52 ± 3.17	NT	8.56 ± 2.61	NT
6b	10.49 ± 2.49	18.49 ± 9.18	3.58 ± 1.06	NT
6c	25.23 ± 9.68	46.91 ± 1.99	6.74 ± 1.30	NT
7a	8.03 ± 1.23	4.66 ± 0.28	4.30 ± 0.99	1.77 ± 0.39
7b	12.86 ± 1.27	NT	7.82 ± 0.87	29.72 ± 1.98
7e	28.76 ± 3.72	36.64 ± 1.70	9.33 ± 0.82	116.25 ± 1.91
7f	12.86 ± 1.28	NT	7.82 ± 0.88	29.72 ± 1.98
7g	4.93 ± 1.69	3.53 ± 0.44	5.48 ± 0.81	1.43 ± 0.14
7j	4.76 ± 0.60	31.94 ± 9.19	1.83 ± 0.52	15.00 ± 0.77
7k	24.01 ± 6.15	15.19 ± 8.81	12.88 ± 1.15	NT
7l	8.99 ± 2.60	7.72 ± 0.76	2.97 ± 0.65	2.25 ± 0.31
7m	4.08 ± 1.21	3.88 ± 0.66	1.86 ± 0.39	1.73 ± 0.18
7n	5.72 ± 0.87	24.85 ± 3.54	3.41 ± 1.60	3.82 ± 0.32
7o	27.65 ± 5.00	18.70 ± 5.82	13.95 ± 2.89	NT
7p	6.93 ± 0.58	4.69 ± 1.18	2.26 ± 0.55	2.81 ± 0.31
7q	6.89 ± 0.86	33.37 ± 8.92	1.73 ± 0.25	6.89 ± 0.86
Sorafeni[b]	23.01 ± 1.32	16.69 ± 4.44	13.62 ± 0.52	12.33 ± 2.52

Abbreviations: NT, not tested.
[a]The average of three trials.
[b]Commercial sorafenib was used as positive control.

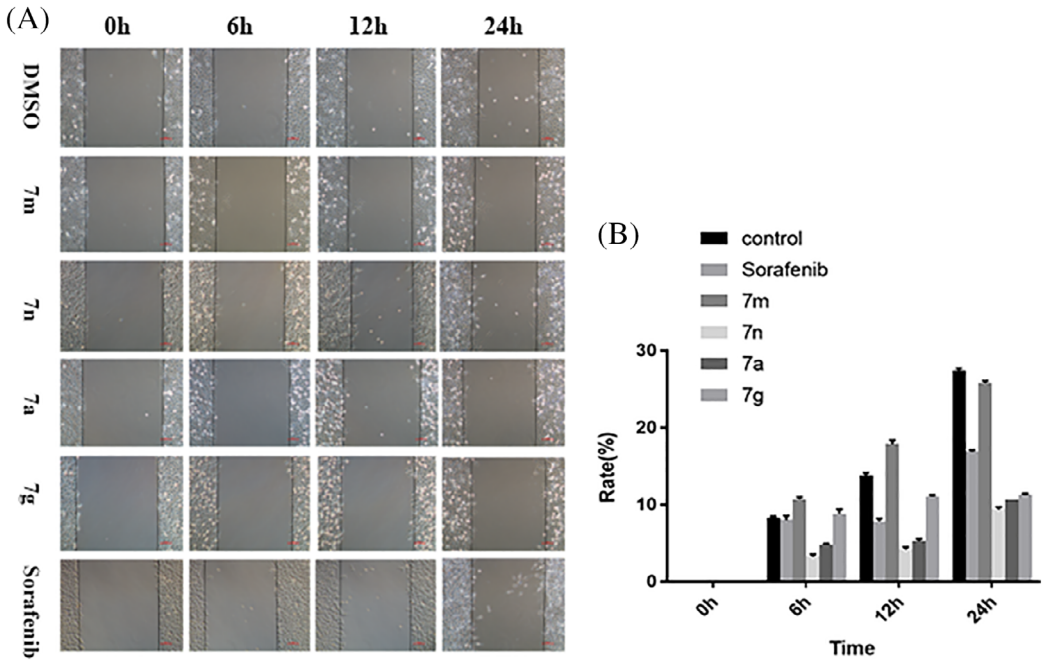

FIGURE 3 A, The picture of wound healing (10× magnification). B, The migration ratios of A549

Significant closure of the scratch wound was observed for the control group after 24 hours. However, scratch wound closure was significantly inhibited in the **7g** group, showing a defect in cell migration following stimulating with **7g** (Figure 3).

2.4 | Apoptosis evaluation by flow cytometry

To investigate the function of potential compounds in cell apoptosis, flow cytometry assay was conducted. As shown in (Figure 4A,B), all of the hopeful compounds induced cell apoptosis in A549 and PC-3 cells in different concentration (5, 10, and 20 μM). These data hasted that as the concentration increasing, the compounds increasingly induced A549 and PC-3 cells apoptosis, as compared with the control group (Figure 4C,D). The apoptosis ratios (including the early and late apoptosis rates) of A549 and PC-3 were remarkable influenced by **7g** in a dose-dependent manner. The apoptosis ratios of treatment with **7g** were significantly increased (from 50.0% to 55.9% against A549, from 53.1% to 69.9% against PC-3) compared with sorafenib groups (from 12.9% to 33.0% against A549, from 25.4% to 53.1% against PC-3).

2.5 | Western blot

At last, the functions of **7g** in the expression and activity of EGFR was estimated through adopting the western blot assay. In Figure 5, phosphorylated EGFR (Tyr1068) and EGFR protein levels were hindered by **7g** management at the concentrations of 5 μM. Unlike sorafenib, **7g** inhibited cell growth by suppressing the activity of EGFR, especially the expression of p-EGFR (Tyr1068).

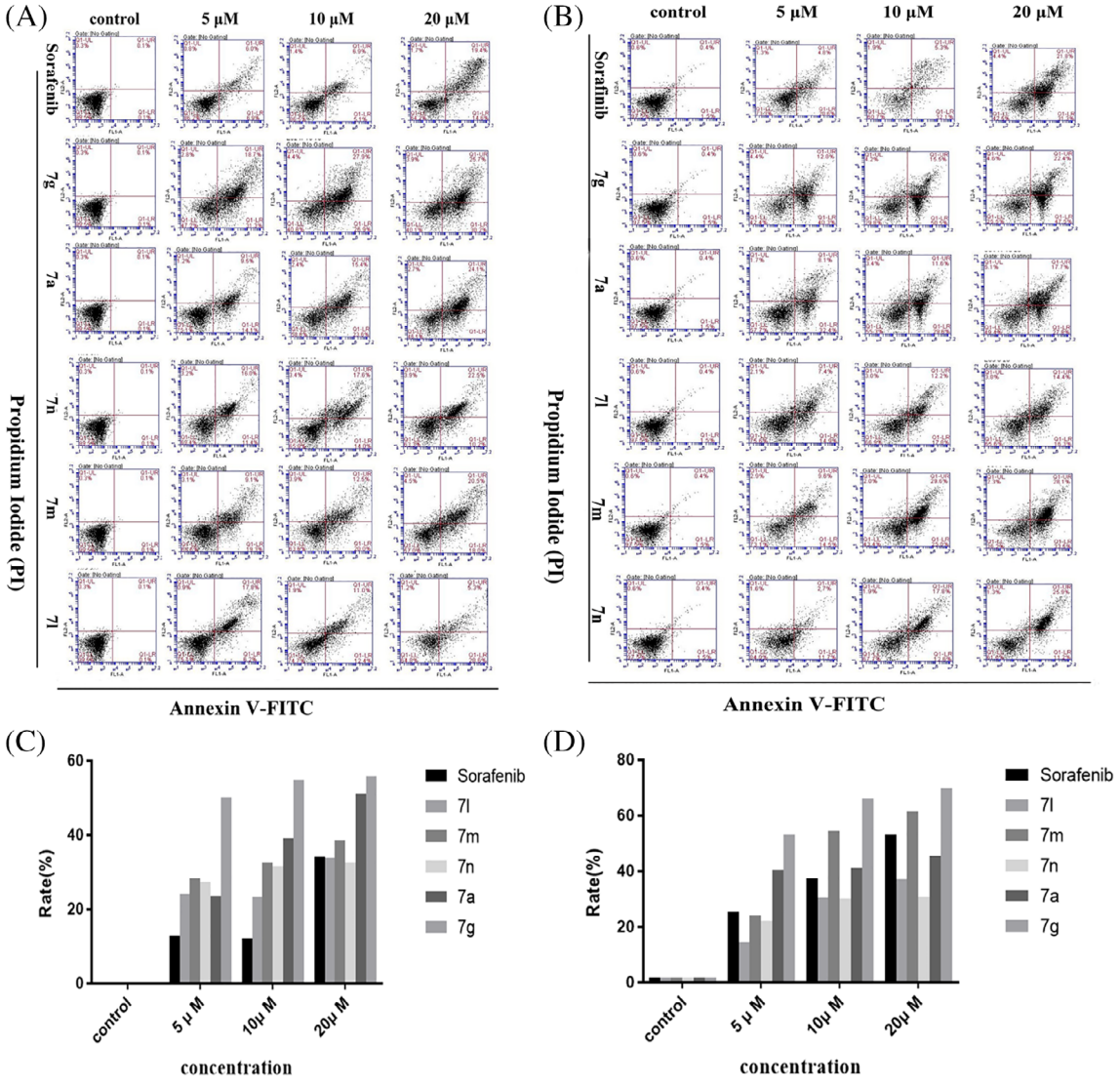

FIGURE 4 A, Annexin/PI statin of A549. B, Annexin/PI statin of PC-3. C, The apoptosis rate of A549. D, The apoptosis rate of PC-3

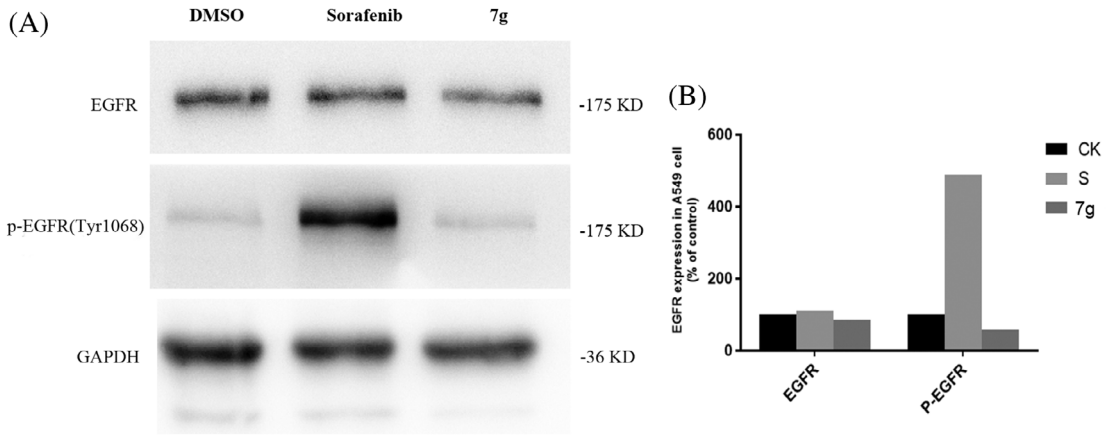

FIGURE 5 A, Detection of EGFR expression in A549 by western blot. B, The statistical results

3 | CONCLUSIONS

In conclusion, a series of sorafenib derivatives containing indole (ketone) semicarbazide analogues were designed and synthesized. Further, the biological activities of these compounds were evaluated according to the MTT method, wound healing assay, flow cytometry and western blot analysis. Compound **7g** with the excellent activity could be promising lead candidate for the following research.

4 | EXPERIMENTAL SECTION

4.1 | Materials and methods

All reagents were purchased from commercial sources as analytical grade and were used without further purification. All reactions were monitored by thin-layer chromatography (TLC). ^{1}H NMR and ^{13}C NMR spectra were performed on a Bruker Ascend 400 NMR spectrometer and JEOL-ECX 500 NMR spectrometer (except for the ^{1}H NMR spectra of **7l** was measured on a Bruker Avance spectrometer at 600 MHz) using deuterated dimethyl sulfoxide (DMSO-d_6) as solvent and TMS as internal standard. Chemical shifts were expressed as δ ppm and coupling constants were given as J Hz. High-resolution mass spectra (HRMS) were recorded on Thermo Scientific Q Extractive series with an ESI source. Melting points (°C) were obtained on an X-4D Micro melting point apparatus and were uncorrected.

4.2 | General procedure for the synthesis of 2a–d

To a solution of **1a–b** (55.68 mmol) in anhydrous acetone (225 mL), K_2CO_3 (61.25 mmol) and bromoethane or bromopropane (61.25 mmol) were added. After the mixture was tempestuously stirred and refluxed at 60°C for 10 hours. After finish of the reaction, filtered fleetly and washed twice by acetone, then the filtrate was dried under reduced pressure. The residue was stirred for 30 minutes after adding water, then ultrasonicated for 2 minutes, filtered, dried, and recrystallized from methanol to gain compounds **2a–d**.

4.3 | General procedure for the synthesis of 4a–i

To a solution of substituted aniline **3a–i** (50 mmol) in anhydrous acetone (50 mL), K_2CO_3 (13.8 g, 0.100 mol) was added, and phenyl carbonochloridate (50 mmol) was distributed droplets in the mixture keeping the temperature between 0°C and5°C, then the mixture was vigorously stirred at room temperature. After completion of the reaction, as captured by TLC, the solvent was evaporated to dryness under reduced pressure. The residue was washed three times by water, filtered, and dried to obtain the corresponding intermediates **4a–i**.

4.4 | General procedure for the synthesis of 6a–c and 7a–q

The key intermediates **5a–i** (3.05 mmol) and various indole (ketone) derivatives substituted isatins or **2a–d** (3.36 mmol) were dissolved in CH_3CH_2OH (10 mL) at room temperature, then catalytic amount of sulfuric acid (0.15 mmol) were dropwise added to the solution, and monitored by TLC (PE: EA = 1:4). After the reaction was finished, the mixture was cooled to room temperature and the solid precipitate was filtered, washed with ethanol (5 mL × 2), dried, and purified by recrystallization

using methanol to yield the target compounds **6a–c** and **7a–q**.

4.5 | *N*-(4-chloro-3-(trifluoromethyl) phenyl)-2-(2-oxoindolin-3-ylidene) hydrazine -1-carboxamide (6a)

Yellow solid, yield: 69.78%, mp 260°C-261°C; ^{1}H NMR (500 MHz, DMSO-d_6) δ 10.77 (s, 1H, CONHN), 10.54 (s, 1H, indoloneNH), 9.96 (s, 1H, PhNHCO), 8.15 (d, J = 2.5 Hz, 1H, HAr), 8.04 (d, J = 7.6 Hz, 1H, HAr), 7.88 (dd, J = 8.8, 2.5 Hz, 1H, HAr), 7.64 (d, J = 8.8 Hz, 1H, HAr), 7.35 (td, J = 7.7, 0.8 Hz, 1H, HAr), 7.07-7.01 (m, 1H, HAr), 6.88 (d, J = 7.8 Hz, 1H, HAr).^{13}C NMR (101 MHz, DMSO-d_6) δ 165.15, 153.24, 143.76, 138.77, 136.25, 132.72, 132.52 (d, J = 3.6 Hz), 125.99, 124.11, 124.08, 123.56, 123.43 (q, J = 275.73 Hz), 121.89, 118.66 (dd, J = 4.4, 1.9 Hz), 115.95, 111.05. HRMS (ESI) *m/z*calcd for $C_{16}H_{10}ClF_3N_4O_2$ $[M\text{-}H]^+$ 381.03606, found 381.03729.

4.6 | *N*-(3,4-difluorophenyl)-2-(2-oxoindolin-3-ylidene)hydrazine-1-carboxamide(6b)

Yellow powder, yield: 69.55%, mp 253°C-254°C; ^{1}H NMR (500 MHz, DMSO-d_6) δ 10.80 (s, 1H, CONHN), 10.50 (s, 1H, indoloneNH), 9.74 (s, 1H, PhNHCO), 8.08 (d, J = 7.6 Hz, 1H, HAr), 7.83-7.74 (m, 1H, HAr), 7.44-7.33 (m, 3H, HAr), 7.09 (t, J = 7.5 Hz, 1H, HAr), 6.92 (d, J = 7.8 Hz, 1H, HAr). ^{13}C NMR (101 MHz, DMSO-d_6) δ 165.22, 153.10, 146.77, 143.67, 143.63, 136.19 (dd, J = 9.5, 2.4 Hz), 135.80, 132.60, 125.88, 122.14, 117.93 (d, J = 18.0 Hz), 116.21 (dd, J = 5.5, 3.2 Hz), 115.99, 111.04, 108.90 (d, J = 21.6 Hz). HRMS (ESI) *m/z*calcd for $C_{15}H_{10}F_2N_4O_2$ $[M\text{-}H]^+$ 315.06881, found 315.06952.

4.7 | *N*-(4-chloro-3-(trifluoromethyl) phenyl)-2-(5-methyl-2-oxoindolin-3-ylidene)hydrazine-1-carboxamide(6c)

Orange yellow powder, yield: 70.00%, mp 250°C-252°C; ^{1}H NMR (500 MHz, DMSO-d_6) δ 10.68 (s, 1H, CONHN), 10.56 (s, 1H, indoloneNH), 9.90 (s, 1H, PhNHCO), 8.21 (d, J = 2.6 Hz, 1H, HAr), 7.97-7.92 (m, 2H, HAr), 7.68 (d, J = 8.8 Hz, 1H, HAr), 7.20 (dd, J = 7.9, 0.7 Hz, 1H, HAr), 6.81 (d, J = 7.9 Hz, 1H, HAr), 2.33 (s, 3H, Ph-CH3). ^{13}C NMR (101 MHz, DMSO-d_6) δ 165.17, 153.38, 141.50, 138.76, 136.34, 133.01, 132.50, 131.13, 127.31 (d, J = 2.5 Hz), 127.00 (d, J = 2.5 Hz), 126.49, 123.01 (q, J = 272.7 Hz), 121.67, 118.81 (q, J = 5.4 Hz), 116.03, 110.73, 21.05. HRMS (ESI) *m/z*calcd for $C_{17}H_{12}ClF_3N_4O_2$ $[M\text{-}H]^+$ 395.05171, found 395.05276.

4.8 | 2-((1*H*-indol-3-yl)methylene)-*N*-(3-bromophenyl)hydrazine-1-carboxamide(7a)

Off-white powder, yield: 45.36%, mp 214°C-215°C; ^{1}H NMR (500 MHz, DMSO-d_6) δ 11.52 (s, 1H, indoleNH), 10.44 (s, 1H, CONHN), 8.72 (s, 1H, PhNHCO), 8.18 (d, J = 7.5 Hz, 1H, HAr), 8.16 (s, 1H, CH═N, HAr), 8.00 (d, J = 1.9 Hz, 1H, HAr), 7.79 (d, J = 2.7 Hz, 1H, indole-2-CH), 7.58-7.54 (m, 1H, HAr), 7.40 (d, J = 7.8 Hz, 1H, HAr), 7.23 (t, J = 8.1 Hz, 1H, HAr), 7.19-7.13 (m, 3H, HAr). ^{13}C NMR (101 MHz, DMSO-d_6) δ 153.43, 141.53, 139.63, 137.42, 130.93, 130.11, 125.16, 124.65, 122.94, 122.10, 121.99, 121.94, 120.91, 118.78, 112.24, 111.75. HRMS (ESI) *m/z*calcd for $C_{16}H_{13}BrN_4O$ $[M\text{-}H]^+$ 355.01890, found 355.02020.

4.9 | 2-((1*H*-indol-3-yl)methylene)-*N*-(3,4-difluorophenyl)hydrazine-1-carboxamide(7b)

White powder, yield: 70.12%, mp 213°C-214°C; ^{1}H NMR (500 MHz, DMSO-d_6) δ 11.55 (s, 1H, indoleNH), 10.47 (s, 1H, CONHN), 8.79 (s, 1H, PhNHCO), 8.23 (d, J = 7.6 Hz, 1H, HAr), 8.20 (s, 1H, CH═N), 7.88-7.83 (m, 1H, HAr), 7.83 (d, J = 2.7 Hz, 1H, indole-2-CH), 7.44 (d, J = 7.9 Hz, 2H, HAr), 7.37 (dt, J = 18.4, 9.1 Hz, 1H, HAr), 7.24-7.14 (m, 2H, HAr). ^{13}C NMR (101 MHz, DMSO-d_6) δ153.56, 149.40 (dd, J = 242.1, 13.0 Hz), 145.18 (dd, J = 239.8, 12.5 Hz), 139.69, 137.43, 137.00 (dd, J = 9.4, 2.6 Hz), 130.13, 124.63, 122.95, 122.21, 120.90, 117.51 (d, J = 17.6 Hz), 116.20 (dd, J = 5.5, 3.1 Hz), 112.22, 111.76, 108.83 (d, J = 21.6 Hz). HRMS (ESI) *m/z*calcd for $C_{16}H_{12}F_2N_4O$ $[M\text{-}H]^+$ 313.08954, found 313.09061.

4.10 | 2-((1*H*-indol-3-yl)methylene)-*N*-(4-chloro-3-(trifluoromethyl)phenyl) hydrazine-1-carboxamide(7c)

White needle solid, yield: 75.00%, mp 224°C-225°C; ^{1}H NMR (500 MHz, DMSO-d_6) δ 11.59 (s, 1H, indoleNH), 10.59 (s, 1H, CONHN), 9.09 (s, 1H, PhNHCO), 8.34 (d, J = 2.5 Hz, 1H, HAr), 8.26 (d, J = 7.7 Hz, 1H, HAr), 8.21 (s, 1H, CH═N, HAr), 7.95 (dd, J = 8.8, 2.4 Hz, 1H, HAr), 7.84 (d, J = 2.6 Hz, 1H, indole-2-CH), 7.65 (d, J = 8.8 Hz, 1H, HAr), 7.44 (d, J = 7.9 Hz, 1H, HAr), 7.23-7.18 (m,

1H, HAr), 7.16 (td, J = 7.6, 1.1 Hz, 1H, HAr). ^{13}C NMR (101 MHz, DMSO-d_6) δ 153.53, 139.99, 139.59, 137.41, 132.12, 130.17, 127.05 (d, J = 4.9 Hz), 126.75 (d, J = 3.3 Hz), 126.47, 124.91, 123.42(q, J = 273.71 Hz) 123.13, 122.95, 120.85, 118.61 (dd, J = 10.8, 4.9 Hz), 112.21, 111.72; HRMS (ESI) m/zcalcd for $C_{17}H_{12}ClF_3N_4O$ $[M-H]^+$ 379.05680, found 379.05777.

4.11 | 2-((1*H*-indol-3-yl)methylene)-*N*-(p-tolyl)hydrazine-1-carboxamide(7d)

Yellow needle solid, yield: 45.52%, mp 236°C-237°C; ^{1}H NMR (400 MHz, DMSO-d_6) δ 11.57 (s, 1H, indoleNH), 10.39 (s, 1H, CONHN), 8.49 (s, 1H, PhNHCO), 8.23 (d, J = 2.7 Hz, 1H, HAr), 8.20 (s, 1H, CH═N), 7.83 (d, J = 2.7 Hz, 1H, indole-2-CH), 7.54 (d, J = 8.4 Hz, 2H, HAr), 7.46 (dd, J = 6.4, 1.9 Hz, 1H, HAr), 7.25-7.17 (m, 2H, HAr), 7.13 (d, J = 8.3 Hz, 2H, HAr), 2.27 (s, 3H, Ph-CH_3). ^{13}C NMR (101 MHz, DMSO-d_6) δ 153.61, 139.03, 137.45, 137.10, 131.54, 129.99, 129.49 (2C), 124.61, 122.93, 121.96, 120.92, 119.87 (2C), 112.29, 111.85, 20.87. HRMS (ESI) m/zcalcd for $C_{17}H_{16}N_4O$ $[M-H]^+$ 291.12404, found 291.12534.

4.12 | 2-((2-chloro-1*H*-indol-3-yl) methylene)-*N*-(3,4-difluorophenyl) hydrazine-1-carboxamide(7e)

Light yellow powder, yield: 70.58%, mp 207°C-208°C; ^{1}H NMR (400 MHz, DMSO-d_6) δ 12.40 (s, 1H, indoleNH), 10.63 (s, 1H, CONHN), 8.83 (s, 1H, PhNHCO), 8.30 (dd, J = 6.7, 1.9 Hz, 1H, HAr), 8.23 (s, 1H, CH═N, HAr), 7.85 (ddd, J = 13.5, 7.5, 2.4 Hz, 1H, HAr), 7.48-7.31 (m, 3H, HAr), 7.29-7.18 (m, 2H, HAr). ^{13}C NMR (101 MHz, DMSO-d_6) δ 153.43, 149.40 (dd, J = 242.2, 13.2 Hz), 145.29 (dd, J = 240.0, 12.8 Hz), 137.16, 136.87 (dd, J = 9.2, 2.7 Hz), 135.43, 126.88, 124.29, 123.54, 122.05, 121.69, 117.50 (d, J = 17.6 Hz), 116.41 (dd, J = 5.6, 3.2 Hz), 111.52, 109.04 (d, J = 21.5 Hz), 107.47. HRMS (ESI) m/zcalcd for $C_{16}H_{11}ClF_2N_4O$ $[M-H]^+$ 347.05057, found 347.05157.

4.13 | 2-((2-chloro-1*H*-indol-3-yl) methylene)-*N*-(3-chlorophenyl)hydrazine-1-carboxamide(7f)

Light yellow powder, yield: 51.25%,mp 223°C-225°C; ^{1}H NMR (500 MHz, DMSO-d_6) δ 12.39 (s, 1H, indoleNH), 10.64 (s, 1H, CONHN, HAr), 8.80 (s, 1H, PhNHCO), 8.27 (dd, J = 6.7, 1.7 Hz, 1H, HAr), 8.20 (s, 1H, CH═N), 7.87 (t, J = 2.0 Hz, 1H, HAr), 7.55 (d, J = 8.2 Hz, 1H, HAr), 7.38-7.30 (m, 2H, HAr), 7.23 (tdd, J = 8.5, 7.2, 1.3 Hz, 2H, HAr), 7.07 (dd, J = 7.9, 2.0 Hz, 1H, HAr). ^{13}C NMR (101 MHz, DMSO-d_6) δ 153.32, 141.27, 137.11, 135.41, 133.39, 130.61, 126.88, 124.28, 123.56, 122.40, 121.99, 121.72, 119.35, 118.57, 111.54, 107.45. HRMS (ESI) m/zcalcd for $C_{16}H_{12}Cl_2N_4O$ $[M-H]^+$ 345.03044, found 345.03140.

4.14 | *N*-(3-bromophenyl)-2-((2-chloro-1*H*-indol-3-yl)methylene)hydrazine-1-carboxamide(7g)

Yellow powder, yield: 42.35%, mp 214°C-215°C; ^{1}H NMR (500 MHz, DMSO-d_6) δ 11.55 (s, 1H, indoleNH), 10.47 (s, 1H, CONHN), 8.75 (s, 1H, PhNHCO), 8.19 (s, 1H), 8.03 (t, J = 1.9 Hz, 1H, HAr), 7.83 (d, J = 2.7 Hz, 1H, HAr), 7.59 (dd, J = 8.2, 0.9 Hz, 1H, HAr), 7.44 (d, J = 8.0 Hz, 1H, HAr), 7.27 (t, J = 8.0 Hz, 1H, HAr), 7.22-7.15 (m, 3H, HAr). ^{13}C NMR (101 MHz, DMSO-d_6) δ 153.45, 141.54, 139.64, 137.43, 130.92, 130.13, 125.17, 124.65, 122.96, 122.13, 122.02, 121.96, 120.92, 118.79, 112.26, 111.76. HRMS (ESI) m/z calcd for $C_{16}H_{12}BrClN_4O$ $[M+Na]^+$ 412.97752, found 412.97845.

4.15 | 2-((2-chloro-1*H*-indol-3-yl) methylene)-*N*-(4-methoxyphenyl) hydrazine-1-carboxamide(7h)

Off-white solid, yield: 68.78%, mp 202°C-203°C; ^{1}H NMR (400 MHz, DMSO-d_6) δ 12.37 (s, 1H, indoleNH), 10.47 (s, 1H, CONHN), 8.43 (s, 1H, PhNHCO), 8.26 (d, J = 7.1 Hz, 1H, HAr), 8.20 (s, 1H, CH═N), 7.52 (d, J = 8.9 Hz, 2H, HAr), 7.37 (d, J = 7.1 Hz, 1H, HAr), 7.30-7.15 (m, 2H, HAr), 6.91 (d, J = 8.9 Hz, 2H, HAr), 3.74 (s, 3H, $PhOCH_3$). ^{13}C NMR (101 MHz, DMSO-d_6) δ 155.43, 153.69, 136.30, 135.44, 132.57, 126.55, 124.32, 123.51, 122.11(2C), 121.82, 121.69, 114.24(2C), 111.56, 107.58, 55.66. HRMS (ESI) m/zcalcd for $C_{17}H_{15}ClN_4O_2$ $[M-H]^+$ 341.07998, found 341.08112.

4.16 | 2-((2-chloro-1*H*-indol-3-yl) methylene)-*N*-(4-chloro-3-(trifluoromethyl) phenyl)hydrazine-1-carboxa-mide(7i)

White solid, yield: 50.00%, mp 232°C-233°C; ^{1}H NMR (500 MHz, DMSO-d_6) δ 12.37 (s, 1H, indoleNH), 10.67 (s, 1H, CONHN), 9.07 (s, 1H, PhNHCO), 8.28 (dd, J = 4.8, 2.2 Hz, 2H, HAr), 8.19 (s, 1H, CH═N), 7.89 (dd, J = 8.8, 2.5 Hz, 1H, HAr), 7.61 (d, J = 8.8 Hz, 1H, HAr), 7.37-7.30 (m, 1H, HAr), 7.22-7.19 (m, 1H, HAr), 7.19-7.15 (m, 1H,

HAr). ^{13}C NMR (101 MHz, DMSO-d_6) δ 153.41, 139.47, 137.54, 135.41, 132.11, 127.41 (d, J = 7.2 Hz), 127.05 (d, J = 3.5 Hz), 126.77, 126.46, 125.12, 123.57, 123.32, 123.30 (q, J = 274.72 Hz), 121.66, 118.80 (q, J = 5.6 Hz), 111.51, 107.44. HRMS (ESI) *m/z*calcd for $C_{17}H_{11}Cl_2F_3N_4O$ $[M-H]^+$ 413.01892, found 413.01907.

4.17 | 2-((2-chloro-1-ethyl-1*H*-indol-3-yl) methylene)-*N*-(4-chloro-3-(trifluoromethyl) phenyl)hydrazine-1-carboxamide(7j)

White powder, yield: 68.74%, mp 230°C-231°C; ^{1}H NMR (400 MHz, DMSO-d_6) δ 10.75 (s, 1H, CONHN), 9.13 (s, 1H, PhNHCO), 8.37 (d, J = 7.6 Hz, 1H, HAr), 8.32 (d, J = 2.5 Hz, 1H, HAr), 8.25 (s, 1H, CH═N), 7.93 (dd, J = 8.8, 2.4 Hz, 1H, HAr), 7.65 (d, J = 8.8 Hz, 1H, HAr), 7.60 (d, J = 8.1 Hz, 1H, HAr), 7.35-7.28 (m, 1H, HAr), 7.28-7.23 (m, 1H, HAr), 4.33 (q, J = 7.1 Hz, 2H, $N\underline{CH_2}CH_3$), 1.30 (t, J = 7.1 Hz, 3H, $NCH_2\underline{CH_3}$). ^{13}C NMR (101 MHz, DMSO-d$_6$) δ 153.38, 139.46, 137.59, 135.38, 132.13, 128.09 (d, J = 5.1 Hz), 127.10 (d, J = 3.2 Hz), 126.79, 126.67, 125.14, 123.34, 123.32123.10 (q, J = 278.76 Hz) 122.41, 118.82 (dd, J = 4.7, 2.3 Hz), 110.46, 107.59, 38.85, 15.12. HRMS (ESI) *m/z*calcd for $C_{19}H_{15}Cl_2F_3N_4O$ $[M-H]^+$ 441.04913, found 441.05048.

4.18 | 2-((2-chloro-1-ethyl-1*H*-indol-3-yl) methylene)-*N*-(4-fluorophenyl)hydrazine-1-carboxamide(7k)

Light pink solid, yield: 67.92%, mp 219°C-221°C; ^{1}H NMR (400 MHz, DMSO-d_6) δ 10.58 (s, 1H, CONHN), 8.65 (s, 1H, PhNHCO), 8.32 (d, J = 7.5 Hz, 1H, HAr), 8.22 (s, 1H, CH═N, HAr), 7.69-7.56 (m, 3H, HAr), 7.36-7.28 (m, 1H, HAr), 7.28-7.23 (m, 1H, HAr), 7.19-7.11 (m, 2H, HAr), 4.32 (q, J = 7.1 Hz, 2H, $N\underline{CH_2}CH_3$), 1.29 (t, J = 7.1 Hz, 3H, $NCH_2\underline{CH_3}$). ^{13}C NMR (101 MHz, DMSO-d_6) δ 158.23 (d, J = 239.5 Hz), 153.57, 136.68, 135.94, 135.35, 127.76, 123.65(2C), 122.20, 122.12 (d, J = 7.6 Hz, 2C), 122.04, 115.49 (d, J = 22.2 Hz, 2C), 110.49, 107.64, 38.81, 15.15. HRMS (ESI) *m/z*calcd for $C_{18}H_{16}ClFN_4O$ $[M-H]^+$ 357.09129, found 357.09250.

4.19 | *N*-(3-bromophenyl)-2-((2-chloro-1-ethyl-1*H*-indol-3-yl)methylene)hydrazine-1-carboxamide(7l)

Pink solid, yield: 69.47%, mp 216°C-217°C; ^{1}H NMR (600 MHz, DMSO-d_6) δ 10.66 (s, 1H, CONHN), 8.79 (s, 1H, PhNHCO), 8.33 (d, J = 7.8 Hz, 1H, HAr), 8.23 (s, 1H, CH═N), 8.01 (t, J = 1.9 Hz, 1H, HAr), 7.59 (dd, J = 12.6, 4.6 Hz, 2H, HAr), 7.33-7.30 (m, 1H, HAr), 7.27 (ddd, J = 7.8, 3.4, 2.0 Hz, 2H, HAr), 7.22-7.18 (m, 1H, HAr), 4.32 (q, J = 7.1 Hz, 2H, $N\underline{CH_2}CH_3$), 1.29 (t, J = 7.2 Hz, 3H, $NCH_2\underline{CH_3}$). ^{13}C NMR (101 MHz, DMSO-d_6) δ 153.27, 141.41, 137.16, 135.37, 130.91, 127.92, 125.32, 125.26, 123.69, 123.66, 122.22, 122.07, 121.91, 118.99, 110.49, 107.62, 38.83, 15.13. HRMS (ESI) *m/z*calcd for $C_{18}H_{16}BrClN_4O$ $[M+H]^+$ 419.02688, found 419.02551.

4.20 | 2-((2-chloro-1-ethyl-1*H*-indol-3-yl) methylene)-*N*-(2-fluorophenyl)hydrazine-1-carboxamide(7m)

Pink solid, yield: 73.58%, mp 205°C-207°C; ^{1}H NMR (400 MHz, DMSO-d_6) δ 10.88 (s, 1H, CONHN), 8.56 (d, J = 2.1 Hz, 1H, PhNHCO), 8.23 (s, 1H, CH═N), 8.22-8.12 (m, 2H, HAr), 7.61 (d, J = 8.2 Hz, 1H, HAr), 7.31 (t, J = 8.4 Hz, 2H, HAr), 7.21 (dt, J = 15.8, 7.7 Hz, 2H, HAr), 7.08 (dd, J = 13.2, 6.2 Hz, 1H, HAr), 4.31 (q, J = 7.0 Hz, 2H, $N\underline{CH_2}CH_3$), 1.28 (t, J = 7.1 Hz, 3H, $NCH_2\underline{CH_3}$). ^{13}C NMR (101 MHz, DMSO-d_6) δ 152.92 (d, J = 241.0 Hz), 152.75, 136.83, 135.45, 128.05, 127.51 (d, J = 10.0 Hz), 125.11, 125.08, 123.71, 123.67, 123.56 (d, J = 7.6 Hz), 122.03, 121.12 (d, J = 12.8 Hz), 115.50 (d, J = 19.0 Hz), 110.83, 107.43, 38.84, 15.11. HRMS (ESI) *m/z*calcd for $C_{18}H_{16}ClFN_4O$ $[M-H]^+$ 357.09129, found 357.09280.

4.21 | 2-((2-chloro-1-ethyl-1*H*-indol-3-yl) methylene)-*N*-(3-fluorophenyl)hydrazine-1-carboxamide(7n)

Milky white powder, yield: 71.70%, mp 210°C-211°C; ^{1}H NMR (400 MHz, DMSO-d_6) δ 10.68 (s, 1H, CONHN), 8.82 (s, 1H, PhNHCO), 8.36-8.28 (m, 1H, HAr), 8.24 (s, 1H, CH═N), 7.66 (dt, J = 12.0, 2.2 Hz, 1H, HAr), 7.58 (d, J = 7.6 Hz, 1H, HAr), 7.46-7.40 (m, 1H, HAr), 7.38-7.24 (m, 3H, HAr), 6.83 (td, J = 8.2, 1.9 Hz, 1H, HAr), 4.31 (q, J = 7.1 Hz, 2H, $N\underline{CH_2}CH_3$), 1.28 (t, J = 7.1 Hz, 3H, $NCH_2\underline{CH_3}$). ^{13}C NMR (101 MHz, DMSO-d_6) δ 162.72 (d, J = 240.4 Hz), 153.27, 141.56 (d, J = 11.4 Hz), 137.07, 135.35, 130.53 (d, J = 9.7 Hz), 127.90, 123.68, 123.66, 122.13 (d, J = 10.0 Hz), 115.74 (d, J = 2.3 Hz), 110.50, 109.08 (d, J = 21.1 Hz), 107.60, 106.68, 106.42, 38.82, 15.13. HRMS (ESI) *m/z*calcd for $C_{18}H_{16}ClFN_4O$ $[M-H]^+$ 357.09129, found 357.09271.

4.22 | 2-((2-chloro-1-ethyl-1*H*-indol-3-yl) methylene)-*N*-(4-methoxyphenyl) hydrazine-1-carboxamide(7o)

Light pink solid, yield: 74.22%, mp 193°C-194°C; ^{1}H NMR (400 MHz, DMSO-d_6) δ 10.47 (s, 1H, CONHN), 8.41 (s, 1H, PhNHCO), 8.30 (d, J = 7.7 Hz, 1H, HAr), 8.22 (s, 1H, CH═N), 7.59 (d, J = 7.9 Hz, 1H, HAr), 7.51 (d, J = 8.9 Hz, 2H, HAr), 7.34-7.22 (m, 2H, HAr), 6.90 (d, J = 8.9 Hz, 2H, HAr), 4.32 (q, J = 6.8 Hz, 2H, N$\underline{CH_2}CH_3$), 3.74 (s, 3H, PhOCH_3), 1.29 (t, J = 7.1 Hz, 3H, NCH$_2\underline{CH_3}$). ^{13}C NMR (101 MHz, DMSO-d_6) δ 155.44, 153.65, 136.32, 135.37, 132.56, 127.60, 123.72, 123.62, 122.12, 122.07, 122.03, 114.37, 114.24(2C), 110.50, 107.73, 55.67, 38.80, 15.14. HRMS (ESI) m/zcalcd for $C_{19}H_{19}ClN_4O_2$ $[M+H]^+$ 371.12693, found 371.12653.

4.23 | 2-((2-chloro-1-ethyl-1*H*-indol-3-yl) methylene)-*N*-(3-chlorophenyl)hydrazine-1-carboxamide (7p)

Light pink powder, yield: 65.37%, mp 203°C-204°C; ^{1}H NMR (400 MHz, DMSO-d_6) δ 10.66 (s, 1H, CONHN), 8.79 (s, 1H, PhNHCO), 8.33 (d, J = 7.3 Hz, 1H, HAr), 8.25 (s, 1H, CH═N), 7.88 (t, J = 1.9 Hz, 1H, HAr), 7.62-7.53 (m, 2H, HAr), 7.36-7.24 (m, 3H, HAr), 7.07 (dd, J = 7.9, 1.3 Hz, 1H, HAr), 4.32 (q, J = 7.1 Hz, 2H, N$\underline{CH_2}CH_3$), 1.30 (t, J = 7.1 Hz, 3H, NCH$_2\underline{CH_3}$). ^{13}C NMR (101 MHz, DMSO-d_6) δ 153.28, 141.26, 137.15, 135.38, 133.41, 130.59, 127.91, 123.71, 123.66, 122.41, 122.21, 122.07, 119.36, 118.56, 110.49, 107.62, 38.83, 15.13. HRMS (ESI) m/zcalcd for $C_{18}H_{16}Cl_2N_4O$ $[M-H]^+$ 373.06174, found 373.06299.

4.24 | *N*-(3-bromophenyl)-2-((2-chloro-1-propyl-1*H*-indol-3-yl)methylene) hydrazine-1-carboxamide(7q)

Off-white solid, yield: 66.28%, mp 222°C-223°C; ^{1}H NMR (400 MHz, DMSO-d_6) δ 10.65 (s, 1H, CONHN), 8.78 (s, 1H, PhNHCO), 8.32 (d, J = 7.4 Hz, 1H, HAr), 8.24 (s, 1H, CH═N), 8.01 (t, J = 1.7 Hz, 1H, HAr), 7.60 (t, J = 6.9 Hz, 2H, HAr), 7.35-7.18 (m, 4H, HAr), 4.26 (t, J = 7.1 Hz, 2H, N$\underline{CH_2}CH_2CH_3$), 1.83-1.70 (m, 2H, NCH$_2\underline{CH_2}CH_3$), 0.87 (t, J = 7.4 Hz, 3H, NCH$_2$CH$_2\underline{CH_3}$). ^{13}C NMR (101 MHz, DMSO-d_6) δ 153.28, 141.41, 137.20, 135.94, 130.92, 128.37, 125.33, 123.63, 123.57, 122.21, 122.16, 122.05, 121.90, 119.00, 110.76, 107.53, 45.21, 23.00, 11.40. HRMS (ESI) m/zcalcd for $C_{19}H_{18}BrClN_4O$ $[M+H]^+$ 433.04253, found 433.04111.

4.25 | MTT assay

Antitumor activities of compounds **6a–c** and **7a–q** against four types of cancer cells named A549, K562, PC-3, and SMMC-7721 were also tested at 10 μM, and assessed according to the method of cell growth rate. The PC-3 was maintained in monolayer culture at 37°C and 5% CO_2 in DMEM medium supplemented with 10% fetal bovine serum and 1% Penicillin Streptomycin. The others were cultured in RPMI1640 supplemented with the same mixtures. The cells that grew well observed by an inverted phase microscope (Nikon Ti-s) were seeded in 96-well plates in 180 μL aliquots at 3×10^4 cells/mL for MTT assays. For each compound, five concentrations (0.625, 1.25, 2.5, 5, and 10 μM) were evaluated and each was done in five copies. The plates were further incubated for 24 hours and the assay was terminated by the addition of 20 μL of 5% MTT and incubated for 4 hours at 37°C. Finally, the supernatant was discarded. The bound amount of stain was subsequently eluted with 150 μL of DMSO and the absorbance was measured with an enzyme-labeled instrument (TECAN infinite M200 PRO) at 490 nm wavelength. The growth percentage was calculated on a plate-by-plate basis for test wells relative to control wells. The sensitivity of the cancer cells to each test compound was expressed in terms of IC_{50}, indicated as mean values ± SD for three independent experiments. Statistical analysis was performed using Graphpad prism version 7 for Student's test. Values of $P < .05$ were considered significant.

4.26 | Wound healing assay

The cells were seeded in six-well plate, and each hole was 1 mL, at 37°C, 5% CO_2 and saturated humidity cell culture medium 24 hours to cell fusion. The 10-μL micropipette was vertically scratched in the six-well plates, and the PBS solution was rinsed two times. The compounds were added and divided into five solutions, each hole was 1 mL, and the negative control group was added with the same volume of cell culture medium. Digital images of the wounded monolayers were obtained by photomicroscope (Ti-S, Nikon) at 0, 6, 12, and 24 hours. The unfilled scratched zones were quantified by Java's Image J software.

4.27 | Apoptosis evaluation by flow cytometry

The A549 cells stimulated by potential compounds was assayed 24 hours later using an Annexin V-fluorescein

isothiocyanate (FITC)/propidium iodide (PI) apoptosis assay. Briefly, cells were incubated with 5 μL Annexin V-FITC (Solabio, Beijing, China) under conditions devoid of light for 15 minutes at 4°C. Next, 5 μL PI was adopted for dying cells for 10 minutes at room temperature. A flow cytometer (C6; BD Biosciences) was used to examine the rate of apoptosis.

4.28 | Western blot

A549 cell was managed with 7 g at 5 μM for 48 hours and sorafenib as the control. After treatment, above cells were laundered three times with PBS to stop the stimulation. Subsequently, these cells were collected and segregated via adopting RIPA lysis buffer (Enzyme-linked, Shanghai, China) with the correlative protease inhibitors (Beyotime, Shanghai, China). The BCA Protein Assay Kit (Beyotime, Shanghai, China) was carried out for determination of total protein concentration. Twenty microliters of protein samples were segregated through utilizing 10% SDS-PAGE, and next transferred onto PVDF membranes and processed for immune blotting with the relevant primary antibodies at 4°C for 200 minutes. The befitting primary antibodies include EGFR (CST11862, 1:800), phosphorylated (p)-EGFR (CST11862, 1:800) and GAPDH (proteintech HRP-60004, 1:20 000) were sealed in Antibody Dilution Buffer (Beyotime, Shanghai, China), and cocultivated with the PVDF membrane at 4°C overnight. After this, the second antibody (proteintech SA00001-2, 1:10 000) was replenished and cofostered with the above membrane for additional 1 hours at room temperature. An enhanced chemiluminescent kit (MilliPore, UK) was then used to conduct chemiluminescent detection.

ACKNOWLEDGMENTS

This study was supported by the project of State Key Laboratory of Functions and Applications of Medicinal Plants, Guizhou Medical University (No. FAMP201707K), and the National Natural Science Foundation of China (No. 21867004), and the Science Technology Program of Guizhou province (No. 20185781).

SUPPORTING INFORMATION

Additional supporting information including ^{1}H, ^{13}C NMR and HRMS spectra of compounds **6a–c** and **7a–q** may be found online in the Supporting Information section at the end of the article.

ORCID

Zhen-Chao Wang https://orcid.org/0000-0003-1859-0128

REFERENCES

[1] J. W. Yao, J. Chen, Z. P. He, W. Sun, W. F. Xu, *Bioorg. Med. Chem.* **2012**, *20*, 2923.
[2] A. Gauthier, M. Ho, *Hepatol. Res.* **2013**, *43*, 147.
[3] G. Ranieri, G. Gadaleta-Caldarola, V. Goffredo, R. Patruno, A. Mangia, A. Rizzo, R. L. Sciorsci, C. D. Gadaleta, *Curr. Med. Chem.* **2012**, *19*, 938.
[4] W. Wu, P. Lu, S. Y. Chen, N. F. Yu, *Acta. Pharm. Sin.* **2009**, *3*, 242.
[5] S. M. Wilhelm, L. Adnane, R. Newell, A. Villanueva, J. M. Llovet, M. Lynch, *Mol. Cancer Ther.* **2008**, *7*, 3129.
[6] S. Wilhelm, C. Carter, M. Lynch, T. Lowinger, J. Dumas, R. A. Smith, B. Schwartz, R. Simantov, S. Kelley, *Nat. Rev.* **2006**, *5*, 835.
[7] L. Liu, Y. Cao, C. Chen, X. Zhang, A. McNabola, D. Wilkie, S. Wilhelm, M. Lynch, C. Carter, *Cancer Res.* **2006**, *66*, 11851.
[8] T. Guida, S. Anaganti, L. Provitera, R. Gedrich, E. Sullivan, S. M. Wilhelm, M. Santoro, F. Carlomagno, *Clin. Cancer Res.* **2007**, *13*, 3363.
[9] L. Adnane, P. A. Trail, I. Taylor, S. M. Wilhelm, *Methods Enzymol.* **2006**, *407*, 597.
[10] M. Rahmani, E. M. Davis, C. Bauer, P. Dent, S. Grant, *J. Biol. Chem.* **2005**, *280*, 35217.
[11] C. Yu, L. M. Bruzek, X. W. Meng, G. J. Gores, C. A. Carter, S. H. Kaufmann, A. A. Adjei, *Oncogene* **2005**, *24*, 6861.
[12] K. F. Chen, W. T. Tai, J. W. Huang, C. Y. Hsu, W. L. Chen, A. L. Cheng, P. J. Chen, C. W. Shiau, *Eur. J. Med. Chem.* **2011**, *46*, 2845.
[13] S. Huang, F. A. Sinicrope, *Mol. Cancer Ther.* **2010**, *9*, 742.
[14] F. Yang, T. E. Van Meter, R. Buettner, M. Hedvat, W. Liang, C. M. Kowolik, N. Mepani, J. Mirosevich, S. Nam, M. Y. Chen, G. Tye, M. Kirschbaum, R. Jove, *Mol. Cancer Ther.* **2008**, *7*, 3519.
[15] A. El-Mekabaty, A. A. Fadda, *J. Heterocyclic Chem.* **2018**, *55*, 2303.
[16] S. Mostafa, M. K. El-Dean Adel, A. Mostafa, H. Reda, *J. Heterocycl. Chem.* **2018**, *55*, 1166.
[17] P. S. Bhale, H. V. Chavan, S. B. Dongare, S. N. Shringare, Y. B. Mule, S. S. Nagane, B. P. Bandgar, *Bioorg. Med. Chem. Lett.* **2017**, *27*, 1502.
[18] V. A. Barbosa, P. Baréa, R. S. Mazia, T. Ueda-Nakamura, W. F. Costa, M. A. Foglio, A. L. Goes Ruiz, J. E. Carvalho, D. B. Vendramini-Costa, C. V. Nakamura, M. H. Sarragiotto, *Eur. J. Med. Chem.* **2016**, *124*, 1093.
[19] K. Milger, N. Kneidinger, C. Neurohr, F. Reichenberger, J. Behr, *Eur. Respir. J.* **2015**, *46*, 1217.
[20] P. Cava-Montesinos, K. Nilles, M. L. Cervera, M. de la Guardia, *Talanta* **2005**, *66*, 895.
[21] A. Afzal, M. S. Thayyil, P. A. Sivaramakrishnan, M. K. Sulaiman, K. S. Hussan, C. Y. Panicker, K. L. Ngai, *J. Non-Cryst. Solids* **2019**, *508*, 33.
[22] M. V. Chatziathanasiadou, E. K. Stylos, E. Giannopoulou, M. H. Spyridaki, E. Briasoulis, H. P. Kalofonos, A. G. Tzakos, *J. Pharm. Biomed.* **2019**, *164*, 690.
[23] W. L. Li, H. H. Sun, F. J. Xu, W. Shuai, J. Liu, S. T. Xu, H. Q. Yao, C. Ma, J. Y. Xu, *Bioorg. Chem.* **2019**, *85*, 49.
[24] W. M. Eldehna, A. M. El Kerdawy, G. H. Al-Ansary, S. T. Al-Rashood, M. M. Ali, A. E. Mahmoud, *Eur. J. Med. Chem.* **2019**, *163*, 37.
[25] D. D. Mukherjee, N. M. Kumar, M. P. Tantak, A. Das, A. Ganguli, S. Datta, D. Kumar, G. Chakrabarti, *Biochemistry* **2016**, *55*, 3020.

[26] J. R. Harrison, C. J. Moody, *Tetrahedron Lett.* **2003**, *44*, 5189.
[27] X. Zhai, G. L. Bao, L. M. Wang, M. K. Cheng, M. Zhao, S. J. Zhao, H. Y. Zhou, P. Gong, *Bioorg. Med. Chem.* **2016**, *24*, 1331.

SUPPORTING INFORMATION

Additional supporting information may be found online in the Supporting Information section at the end of this article.

How to cite this article: Li W, Qi Y-Y, Wang Y-Y, et al. Design, synthesis, and biological evaluation of sorafenib derivatives containing indole (ketone) semicarbazide analogs as antitumor agents. *J Heterocyclic Chem*. 2020;1–13. https://doi.org/10.1002/jhet.3972